THE JOURNAL OF BIOLOGICAL CHEMISTRY VOL. 285, NO. 12, pp. 9090–9099, March 19, 2010

Biochemical and Biological Characterization of a New Oxidized Avidin with Enhanced Tissue Binding Properties

Received for publication, October 29, 2009, and in revised form, January 18, 2010 Published, JBC Papers in Press, January 25, 2010, DOI 10.1074/jbc.M109.080457

Antonio Verdoliva[‡], Piero Bellofiore[‡], Vincenzo Rivieccio[‡], Sergio Catello[‡], Maurizio Colombo[‡], Claudio Albertoni[§], Antonio Rosi[§], Barbara Leoni[§], Anna Maria Anastasi[§], and Rita De Santis[§1]

From the [‡]Research and Development Department, Tecnogen S.p.A., Piana di Monte Verna, 81013 Caserta and the [§]Research and Development Department, Sigma-Tau S.p.A., Pomezia, 00040 Rome, Italy

Chicken avidin and bacterial streptavidin are widely employed *in vitro* for their capacity to bind biotin, but their pharmacokinetics and immunological properties are not always optimal, thereby limiting their use in medical treatments. Here we investigate the biochemical and biological properties of a new modified avidin, obtained by ligand-assisted sodium periodate oxidation of avidin. This method allows protection of biotin-binding sites of avidin from inactivation caused by the oxidation step and delay of avidin clearance from injected tissue by generation of aldehyde groups from avidin carbohydrate moieties. Oxidized avidin shows spectroscopic properties similar to that of native avidin, indicating that tryptophan residues are spared from oxidation damage. In strict agreement with these results, circular dichroism and isothermal titration calorimetry analyses confirm that the ligand-assisted oxidation preserves the avidin protein structure and its biotin binding capacity. *In vitro* cell binding and *in vivo* tissue residence experiments demonstrate that aldehyde groups provide oxidized avidin the property to bind cellular and interstitial protein amino groups through Schiff's base formation, resulting in a tissue half-life of 2 weeks, compared with 2 h of native avidin. In addition, the efficient uptake of the intravenously injected ^{111}In-Biotin-DOTA (ST2210) in the site previously treated with modified avidin underlines that tissue-bound oxidized avidin retains its biotin binding capacity *in vivo*. The results presented here indicate that oxidized avidin could be employed to create a stable artificial receptor in diseased tissues for the targeting of biotinylated therapeutics.

Chicken avidin and bacterial streptavidin are tetrameric proteins containing four identical subunits (homotetramer), each of which can bind to biotin (vitamin B_7 and vitamin H) with a high degree of affinity and specificity. The dissociation constant of the (strept)avidin-biotin system is measured to be $K_D = \approx 10^{-15}$ M, making it one of the strongest known noncovalent bonds (1). The high affinity, tetravalency, and stability for biotin have made possible the use of the (strept)avidin-biotin system as a probe and affinity tag in a wide variety of applications in the life sciences (2). These (strept)avidin-biotin techniques are also found to be useful in medical applications *in vivo* to localize and image cancer cells and to pretarget drugs to tumors (3–6). In addition, the use of avidin to neutralize the anticoagulant activity of idrabiotaprinux by increasing the plasma clearance of the idrabiotaprinux-avidin complex has been demonstrated (7).

Despite the fact that avidin and streptavidin are structurally and functionally analogous proteins, they differ in their primary amino acid sequence, pI, glycosylation (8), and immunological reactivity (9). Avidin contains twice the number of the basic amino acids lysine and arginine compared with streptavidin; therefore, the pI of avidin is very high (approximately 10.5), whereas streptavidin has a slightly acidic pI (approximately 6). Each avidin monomer has one *N*-linked carbohydrate side chain, and ~10% of the mass of avidin is due to its carbohydrates mannose and *N*-acetylglucosamine (10, 11). These sugars are not necessary for the stability and the high binding affinity of avidin for biotin (12), but they influence the *in vivo* avidin biodistribution because of their binding to sugar receptors present throughout the reticuloendothelial system (13–16). Streptavidin is void of carbohydrates. Because of these dissimilarities, the plasma half-life and biodistribution of avidin and streptavidin are rather different (17–19). The plasma half-life of avidin is shorter when compared with that of streptavidin (20, 21). Both the positive net charge and its carbohydrates play a role in the rapid blood clearance of avidin and its accumulation in the liver, spleen, and kidneys (22). Streptavidin, on the other hand, accumulates mainly in the kidney (23). In addition, avidin and streptavidin, being xenogenic in human, may stimulate, like other xenogenic therapeutic proteins, an immunological response, thus limiting their repeated use (24–26).

To overcome these immunological and pharmacokinetic problems, chemically modified forms of avidin and streptavidin have been developed. Rosebrough and Hartley (19) deglycosylated and chemically lowered the pI of avidin and attached galactose to streptavidin to modify their pharmacokinetics. Subsequently, Chinol *et al.* (27) succeeded in reducing the immunological response and increasing the plasma half-life of avidin by its poly(ethylene glycol)ylation and succinylation. Several other recent reports have also described genetically modified or new egg white avidins, which should offer advantages over native chicken protein (28–34).

In the perspective of improving avidin pharmacokinetic properties for tissue engineering applications, an oxidized avidin has been recently described showing that, once injected in tissues, might be useful in taking up intravenously injected radioactive biotin (35). Here we describe in detail the procedure for obtaining such an avidin variant by sodium periodate oxidation of the sugar pyranosydic rings after saturation with the

[1] To whom correspondence should be addressed: Sigma-Tau SpA R & D, Via Pontina Km 30.400, Pomezia, 00040 Rome, Italy. Tel.: 390691394283; Fax: 390691393988; E-mail: rita.desantis@sigma-tau.it.

low affinity ligand 4-hydroxyazobenzene-2′-carboxylic acid (HABA)[2] (36). This reaction produces reactive aldehyde groups (CHO) that are virtually inert at acidic pH and, when injected in a tissue, because of the physiological pH, react with NH_2 groups on tissue proteins, delaying clearance of such modified avidin, named $OXavidin_{HABA}$. Here we report the physico/chemical and biological characterization of oxidized avidins by UV, size exclusion chromatography, circular dichroism, isothermal titration calorimetry, cytofluorimetry, and *in vivo* experiments. The results indicate that the HABA-assisted oxidation substantially preserves the structure and the biotin binding property of native avidin, which acquires the capacity to reside within injected tissues for weeks as a consequence of the chemical reaction of aldehyde groups with tissue protein amino groups by Schiff's base formation. The use of native avidin, injected during surgery in the tissue surrounding an excised breast tumor, followed by intravenous radioactive biotin within the next 24 h, has been recently applied in the clinic to prevent local tumor recurrences. This method, named intraoperative avidination for radionuclide treatment (IART®) (37–39), is an innovative way to perform pretargeted tissue radiotherapy, but it is conditioned by the short tissue half-life of native avidin that, diffusing from the injected breast into liver and kidney, requires the blocking of the radioactive biotin uptake in these organs that is performed by injecting human biotinylated albumin (HSAbiot) 10 min before radioactive biotin. The present data confirm that $OXavidin_{HABA}$, being stable in injected tissues, could be a valid alternative to native avidin in IART®. Moreover, it could be employed for other medical applications where a stable artificial receptor in diseased tissues could be envisaged to direct biotinylated therapeutics.

EXPERIMENTAL PROCEDURES

Avidin Oxidation—Native chicken avidin (BioSPA) was incubated, at the final concentration of 3 mg/ml, with sodium periodate, varying from 0 to 40 mM, to oxidize sugars as described previously (40) in 100 mM acetate buffer at pH 5.5 for 1 h at room temperature in the presence or absence of HABA (Sigma). At the end of incubation, oxidized avidin was loaded on a Sephadex™ G-25 fine desalting column (GE Healthcare) and formulated in 100 mM acetate buffer, pH 5.5. To provide complete removal of sodium periodate and HABA, a maximum sample volume of 5% of the total column volume is recommended.

The amount of aldehyde groups generated by oxidation of the sugars was evaluated using the reaction of aldehydes with Purpald® (4-amino-3-hydrazino-5-mercapto-1,2,4-triazole,4-amino-5-hydrazino-4H-1,2,4-triazole-3-thiol), described by Quesenberry and Lee (41). Blocking of CHO groups was performed by reacting avidin with 50–200 mM semicarbazide (Sigma). The biotin binding activity of avidin was measured according to the HABA method (36).

Isothermal Titration Calorimetry—All of the avidins were extensively dialyzed against 100 mM acetate buffer, pH 5.5, the identical buffer in which ST2210 (biotinDOTA) (42) was solubilized, and all of the solutions were degassed prior to use. Titrations were carried out using 10-μl injections given every 5 min. The concentration of ST2210 in the syringe was 18–25 times the concentration of the avidin in the cell; 2.4–2.8 mM ST2210 was titrated into 0.11–0.13 mM avidin. All of the titration data were collected at 25 °C and replicated to determine the experimental standard deviation for each parameter. Binding isotherms were fitted by nonlinear regression using the single-site model provided by Origin software (MicroCal, Inc.). The stoichiometry of the interaction (N), equilibrium association constant (K_A), and change in enthalpy (ΔH) were floated during the fitting of all titration data. The equilibrium dissociation constants (K_D) were calculated as the reciprocal of K_A.

Spectroscopic Analyses—Absorbance spectra in the UV range 240–300 nm were recorded for native and oxidized avidins on a Beckman DU 640 spectrophotometer. The samples were analyzed in 100 mM sodium acetate buffer, pH 5.5, at a final concentration of 0.4–0.5 mg/ml. The far UV CD spectra of native and oxidized avidins were recorded in 100 mM sodium acetate buffer, pH 5.5, with or without 4 equivalents of biotin at 25 °C and at a 4.5 μM concentration using a 1-mm-path length quartz cell. The spectra, from 190 to 260 nm, were acquired by Jasco J-715 spectropolarimeter equipped with a thermostatic water bath. Each spectrum was obtained averaging three scans and subtracting the contribution from the buffer solution. Other experimental settings were: 20 nm $\times$ min^{-1} scan speed, 2.0-nm bandwidth, 0.2-nm resolution, 50-mdeg sensitivity, and 4-s response. The melting curves were recorded by following the decrease of dichroic signal at 225 nm while increasing the temperature in the range of 25–95 °C with the following instrument settings: bandwidth, 1 nm; response, 0.5 s; data pitch, 1 °C; temperature slope, 10 °C/min. Moreover, at every temperature increment of 5 °C a far UV CD spectrum was collected in the experimental conditions reported above. The point of inflection and slope (p) of sigmoidal curves were calculated by means of a Boltzman fitting model of Origin® 7.0 software.

Cell Lines and FACS Analysis—Avidin and streptavidin binding to cells was analyzed by flow cytometry on human tumor cell lines U118MG (glioma) and PC3 (prostate) or murine fibroblasts (3T3), mouse spleen, and red blood cells. The cells were incubated at 37 °C for 2 h in the presence of avidin or streptavidin (5 μg/5 $\times$ 10^5 cells in 100 μl of phosphate-buffered saline), and after washing, the binding was detected by biotin-B-PE (Fluka) 2 μg in 100 μl of phosphate-buffered saline for 1 h at 4 °C. The background was obtained by incubation of cells with biotin-B-PE only. Analysis was performed on a FACScalibur instrument, and the data were elaborated by CellQuest software (Becton Dickinson).

Animals—The care and husbandry of mice were in accordance with the European Directive 86/609 and Italian legislation.

Residency of (Strep)Avidins in Tissue and Uptake of ^{111}In-ST2210—Female Balb/c nude mice (Charles River) were used. The animals were divided in groups of five mice each. ^{125}I radiolabeling of avidin and streptavidin (both from Biospa) was performed with ^{125}Iodine by IODO-GEN™ tubes (Pierce)

[2] The abbreviations used are: HABA, 4′-hydroxyazobenzene-2-carboxylic acid; IART®, intraoperative avidination for radionuclide treatment; HSAbiot, biotinylated human serum albumin; OxidAV, oxidized avidin; $OXavidin_{HABA}$, HABA-protected oxidized avidin; FACS, fluorescence-activated cell sorter; ID, injected dose; PEG, polyethylene glycol.

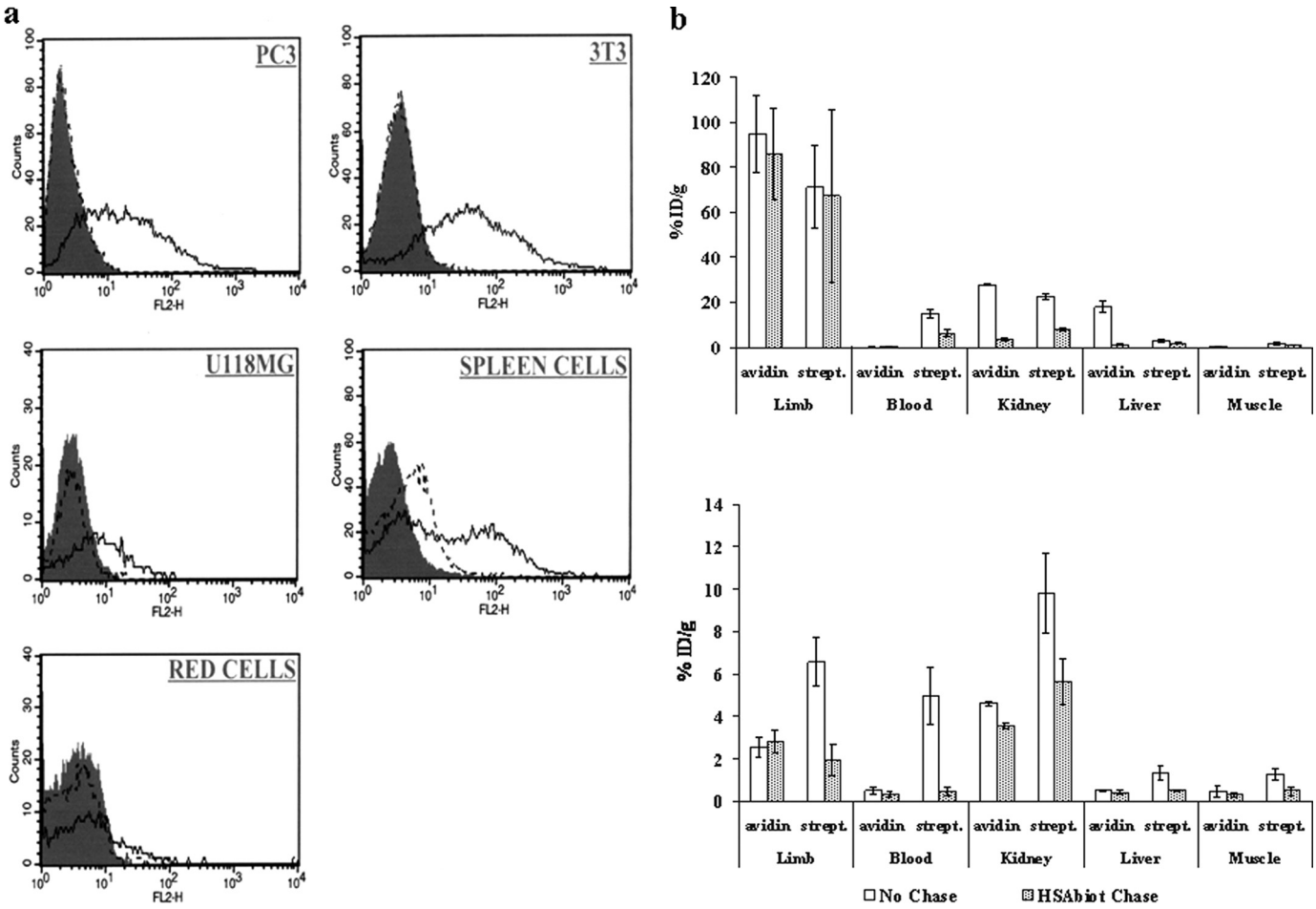

FIGURE 1. ***In vitro* cell binding and *in vivo* uptake of ^{111}In-ST2210 by avidin and streptavidin.** *a*, flow cytometry of human prostate cancer PC3, mouse fibroblast NIH3T3, human glioma U118MG, mouse spleen, and red blood cells. The cells were incubated at 37 °C for 2 h in the presence of avidin (*solid line*) or streptavidin (*dotted line*) and the binding detected by biotin-B-PE. The *gray peaks* represent the background. *b*, uptake of intravenously administered ^{111}In-ST2210 by avidin or streptavidin (*strept.*) 1 (*top panel*) or 24 (*bottom panel*) h after their intramuscular injection in a limb with or without HSAbiot chase. The mice were sacrificed 1 h after ^{111}In-ST2210 injection. The highest uptake of radiolabeled biotin is evident in the treated limb at 1 h but not at 24 h. HSAbiot chase reduces background in nontarget organs. Uptake in controlateral untreated limbs is also indicated (muscle). The data are the averages of five mice, and the *bars* represent the standard deviations.

before periodate oxidation because iodination reaction occurs at pH 7.5, a pH at which intermolecular formation of Schiff's bases of oxidized glycoproteins would occur. ^{125}I-Labeled avidin, streptavidin, or oxidized avidin were injected in one hind limb (tissue avidination) at the dose of 50 μg in ~15 μl of 100 mM sodium acetate, pH 5.5, corresponding to 6×10^5 to 2×10^6 cpm. Groups of mice were sacrificed at the indicated time points. The injected limb and blood, liver, kidney, and controlateral limb were collected and weighed, and radioactivity was quantified by a γ counter (Canberra Packard). Because the weight of the treated tissues was less than 1 g, the data are expressed as the percentages of injected dose/100 mg (% ID/100 mg) of tissue and are the averages of five animals ± S.D. For ^{111}In-Biotin-DOTA uptake, the mice were avidinated as described above and injected intravenously with 16 μg of ^{111}In-ST2210 at the indicated time points. For reducing background, some groups of mice received an intravenous bolus (80 μg) of HSAbiot to block radioactivity uptake in nontarget tissues. This chase step was performed 10 min before ^{111}In-ST2210 intravenous administration. All of the mice were sacrificed 1 h after ^{111}In-ST2210 injection and the avidinated limb, blood, liver, kidney, and controlateral limb were collected and weighed, and radioactivity was quantified by a γ counter (Canberra Packard). The data are expressed as the percentages of injected dose/g (% ID/g) of tissue and are the averages of five mice ± S.D.

RESULTS

Cell Binding and Tissue Kinetics of Avidin and Streptavidin—Looking for a stable receptor for radiolabeled biotin in tissues to be exposed to radiotherapy, preliminary experiments were performed to investigate the *in vitro* cell binding and *in vivo* tissue residence and efficiency in capturing the ST2210 radioactive biotin of both reference molecules avidin and streptavidin. As shown in Fig. 1*a* and as expected from bibliographic data (43), binding of avidin but not streptavidin to a panel of tumor as well as normal cells was confirmed by FACS analysis. Therefore, to evaluate their diffusion kinetics from a treated tissue, either ^{125}I-radiolabeled avidin or streptavidin was injected in the muscle of one hind limb of each mouse, simulating the recently described approach of cancer pretargeted radiotherapy named IART® (37–39), and at different time points the mice were sacrificed, and the treated and controlateral limb (muscle), blood,

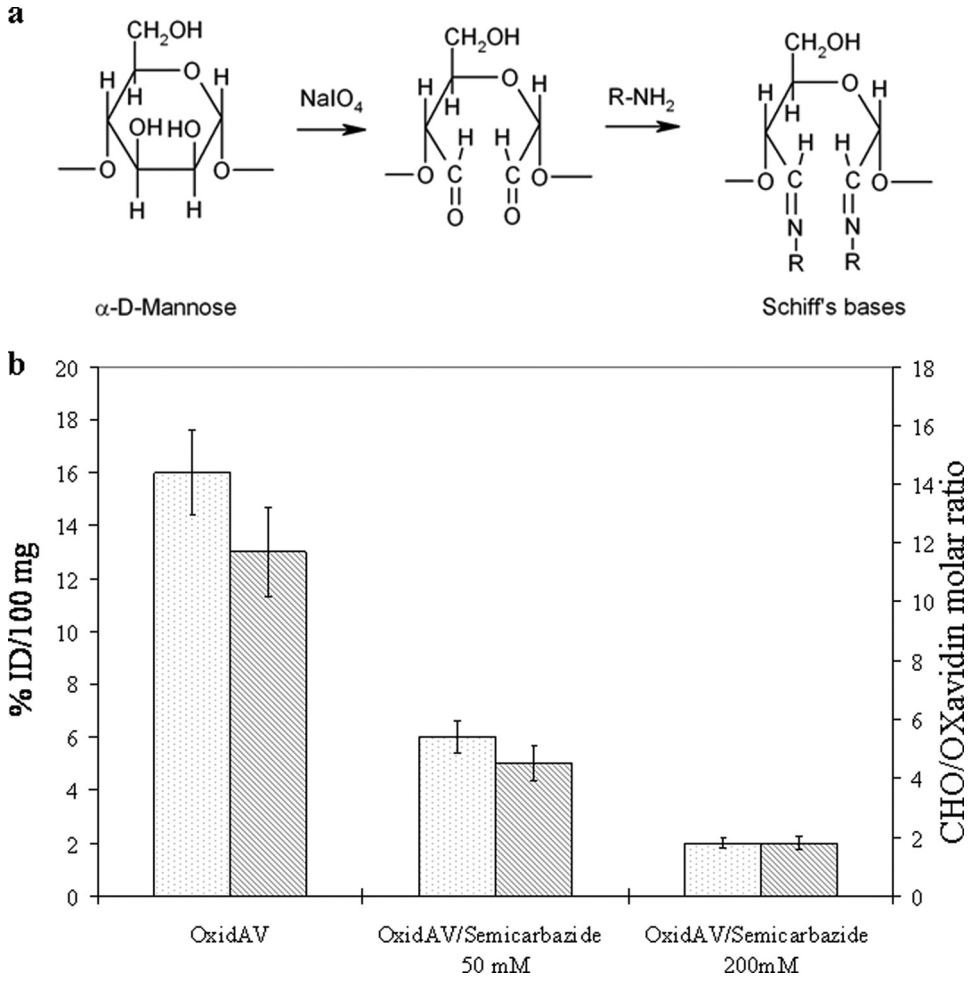

FIGURE 2. *a*, chemical strategy for oligosaccharide oxidation by sodium periodate and Schiff's base formation. *b*, dependence of OxidAV tissue residence on reactive aldehyde groups generated by oxidation with sodium periodate. Tissue residence of oxidized avidin (*white*) is reduced by reduction of its number of CHO groups (*gray*) with 50 or 200 mM semicarbazide. Evaluation was performed 24 h after injection.

TABLE 1

Setting up production method of oxidized avidins

The data are representative of at least three independent determinations. NT, not tested.

Avidin	$NaIO_4$	CHO/avidin	ST2210 binding	Tissue residence 24 h
	mM	*molar ratio ± S.D.*	*% ± S.D.*	*% ID/100 mg ± S.D.*
OxidAV		<LoQ	100[a]	2.1 ± 0.4
	1	5.3 ± 0.6	75.0 ± 0.7	3.1 ± 0.7
	5	7.7 ± 0.7	54.2 ± 2.3	6.3 ± 0.3
	10	8.6 ± 1.3	49.7 ± 2.2	16.0 ± 0.2
	20	12.1 ± 1.3	47.7 ± 2.2	19.2 ± 1.7
	40	9.8 ± 1.8	43.0 ± 1.0	NT
$OXavidin_{HABA}$	10	9.3 ± 1.0	84.0 ± 1.4	16.2 ± 2.3
	20	14.2 ± 2.2	79.3 ± 1.1	19.0 ± 0.2

[a] The experimental value of 97.4 ± 0.5% obtained with ST2210 compared to free biotin by HABA assay is assumed as the 100% reference value for modified avidins.

liver, and kidney were collected, and radioactivity was measured by a γ counter. Previously published data from our group showed that the residence time of ^{125}I-labeled avidin and streptavidin in the treated tissue is very short, with ~8% of the injected dose/100 mg observed after 1 h and less than 1% ID/100 mg after 24 h. In agreement to previous pharmacokinetics data on avidin and streptavidin intravenously injected, the avidin diffused from the injected tissue, exhibited a faster clearance from the blood than streptavidin, and accumulated in the liver and kidney, whereas streptavidin preferentially accumulated in the kidney (35).

Taking into account such diffusion kinetic and biodistribution data, the uptake of radioactive biotin was evaluated in the same mice preinjected with avidin or streptavidin. ^{111}In-ST2210 was intravenously administered 1 or 24 h after tissue avidination, with or without a chasing step with HSAbiot, performed to reduce radioactivity localization in nonavidinated tissues. The Fig. 1*b* (*top panel*) shows that after 1 h from avidin or streptavidin intramuscular injection, the highest ^{111}In-ST2210 localization is in the avidin or streptavidin preinjected limb and kidney. Blood and controlateral limb (muscle) contain less than 0.2% ID/g of tissue, except for the blood of animals treated with streptavidin that contains ~1.5% ID/g of ^{111}In-ST2210 as a consequence of the slower clearance of streptavidin compared with avidin. A clear effect of the HSAbiot chase can be observed in nontarget organs where the nonspecific uptake of radioactive ^{111}In-ST2210, because of the presence of either streptavidin or avidin diffused from the treated limb, is quenched. This shows that the selected chasing condition does not affect the specific radioactivity localization in the treated limb as also shown in the IART® clinical study (38).

In agreement with data of tissue residence, 24 h after tissue avidination the uptake of ^{111}In-ST2210 was very low. In the avidinated limb, as well as in blood, liver, and controlateral limb, the localization of ^{111}In-ST2210 was below 0.5% ID/g of tissue (Fig. 1*b*, *bottom panel*). A higher radioactivity signal was observed in the kidney of mice treated with streptavidin compared with avidin as a consequence of the slower elimination of streptavidin from the circulation.

Oxidized Avidins Production and Characterization—In an attempt to improve the tissue half-life of avidin while reducing its localization in nontarget organs and taking into account that avidin oligosaccharides are not essential for biotin binding, native avidin was chemically modified in the sugar moieties by oxidation with sodium periodate according to the scheme in Fig. 2*a*. This reaction has been widely used since the early 1970s to conjugate *in vitro* glycoproteins to functional protein moieties (40, 44). At acidic pH, the aldehyde groups (CHO) are substantially inert because protein amino groups ($pK_a = 8-9$) are in the protonated NH_3^+ status, but at neutral pH and higher,

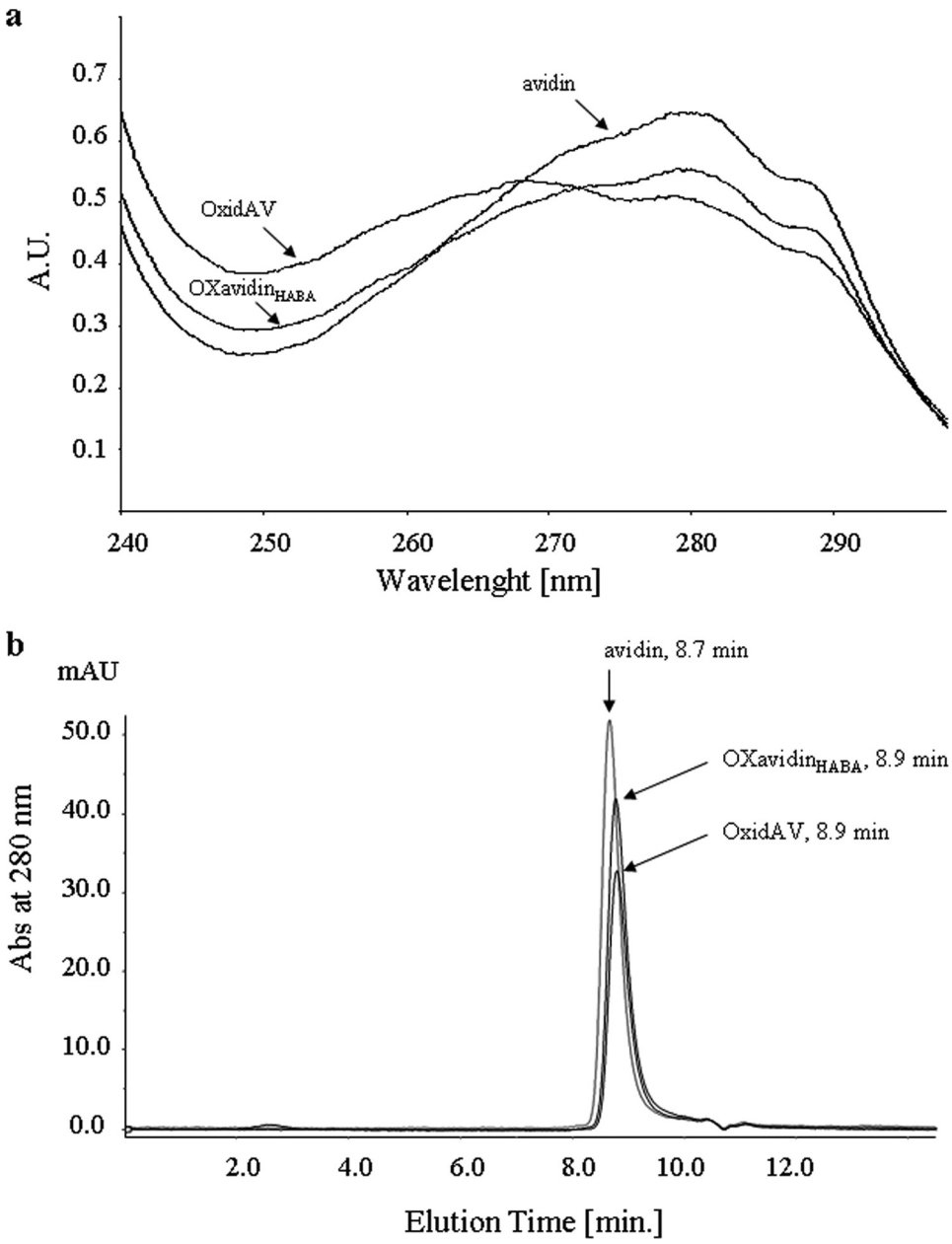

FIGURE 3. *a*, absorption spectra of OxidAV and OXavidin$_{HABA}$, compared with that of the unmodified avidin, in the UV range 240–300 nm. The UV spectrum of OXavidin$_{HABA}$ is similar to that of avidin, whereas that of OxidAV exhibits increased absorbance in the 250–260 nm region, caused by the formation on tryptophan of a substituted oxindole. *b*, size exclusion chromatography analysis of avidin, OxidAV and OXavidin$_{HABA}$ on a BiosepSEC S3000 column. Peaks of oxidized avidins appear slightly delayed compared with the one of avidin, most likely because of modification of hydrodynamic behavior consequent to oligosaccharides oxidation.

aldehyde groups react with protein amino groups to form Schiff's bases.

In a preliminary study performed in a mouse model simulating pretargeted radiotherapy in the muscle, avidin was oxidized with sodium periodate and formulated at pH 5.5 to obtain oxidized avidin. Equal amounts of ^{125}I-labeled oxidized avidin or avidin were then intramuscularly injected in one hind limb of each mouse, and the tissue permanence was evaluated at different time points. One hour after injection, the amount of oxidized avidin in the treated limb was twice that of avidin, and the difference increased with time; avidin was almost undetectable after 24 or 48 h, whereas oxidized avidin was always higher than 10% ID/100 mg of tissue (35). These findings suggested that oxidation allows the avidin to react with tissue proteins *in vivo* by the formation of Schiff's bases.

To investigate the effect of CHO groups on tissue binding and to optimize the oxidation reaction in terms of oxidized avidin (OxidAV) stability and aldehyde groups production, experiments were performed by varying the periodate concentration from 1 to 40 mM, allowing it to react for 1 h at room temperature. The data, collected in Table 1 (OxidAV), indicate that the amount of CHO groups generated by oxidation, and the % ID/100 mg of tissue of OxidAV, after 24 h from injection, increased with the periodate concentration, thus suggesting that the tissue residence of avidin is strictly related to the number of CHO produced. To prove this relationship, ^{125}I-labeled OxidAV (20 mM periodate concentration) was reacted with semicarbazide to block the aldehyde groups, according to the following reaction: avidin-CHO + $NH_2NHCONH_2$ → avidin-CH = $NNHCONH_2$.

Tissue permanence of OxidAV and 50 or 200 mM semicarbazide derivatives, 24 h after intramuscular injection in limb as described previously, was ~16, 6, and 2% ID/100 mg, respectively, indicating a correlation of tissue residence with the number of CHO that were 13, 5, and 2/molecule, respectively (Fig. 2*b*). Nevertheless, gel filtration analyses of oxidized avidins (not shown) indicated that for periodate concentration over 20 mM protein, degradation occurred with significant reduction of its biotin binding capacity, as also determined by HABA test performed with ST2210.

Considering that the tissue permanence of avidin oxidized with 10 and 20 mM $NaIO_4$ at 24 h was ~8–10 times that of avidin, lower or higher periodate concentrations were also tested but discarded for further studies for being either not adequate to generate sufficient CHO groups or too severe to maintain an acceptable level of avidin biological activity.

As previously reported (45), the oxidation with sodium periodate of the sugar pyranosidic rings of avidin is associated to some oxidation of tryptophan amino acidic residues that are known to be important for the biotin binding, thus explain-

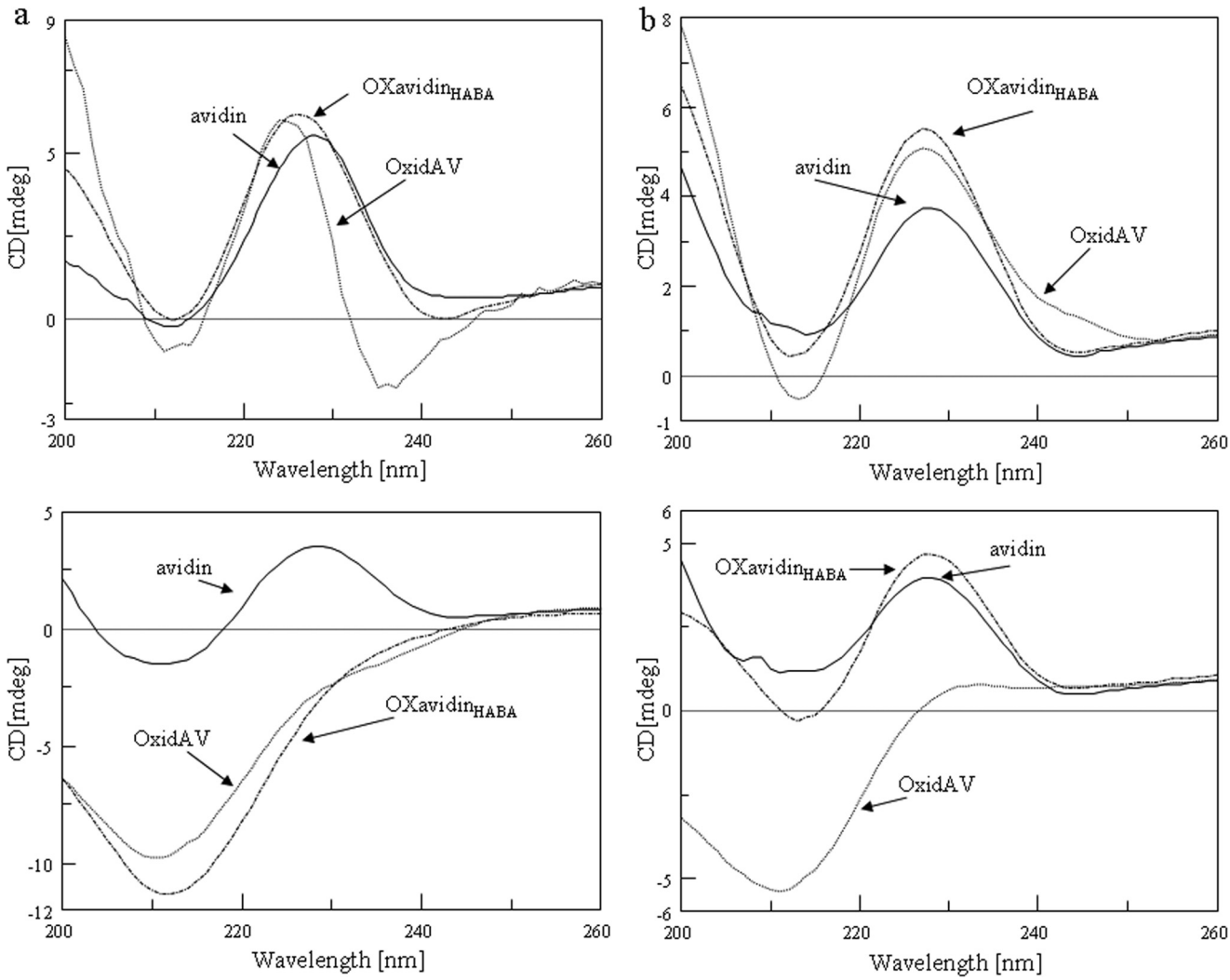

FIGURE 4. **Circular dichroism spectra of native and oxidized avidins.** *a*, CD spectra, recorded at 25 °C (*top panel*), show that OxidAV, and OXavidin$_{HABA}$ lack their secondary structure when heated from 25 to 95 °C (*bottom panel*), if compared with avidin. *b*, the addition of D-biotin stabilizes OXavidin$_{HABA}$ and avidin upon thermal denaturation (*bottom panel*) unlike OxidAV.

ing the reduced ST2210 binding properties of such oxidized avidin. To prevent the damage of the biotin-binding site, the avidin oxidation was performed in the presence of a saturating amount of the low affinity ligand HABA. As shown in Table 1 (OXavidin$_{HABA}$), the protective effect of HABA in avidin oxidation is confirmed by the data of ST2210 binding that show for avidin oxidized with 10 or 20 mM sodium periodate, in the absence (OxidAV) or in the presence of HABA (OXavidin$_{HABA}$), values of ~50 and 80%, respectively compared with ~100% binding capacity of avidin. The data also indicate that the number of CHO groups generated by oxidation and the avidin tissue permanence after 24 h increased with the periodate concentration, thus confirming that the tissue permanence of oxidized avidins is strictly related to the number of CHO groups produced. The oxidized avidins were further characterized for their biochemical and biophysical features.

As reported by Green (45), the extent of tryptophan oxidation is strictly related to the lowering of the characteristic inflections at 282 and 291 nm, whereas the absorbance increases in the 250–260-nm region because of the formation of a substituted oxindole. Analysis of the absorption spectra of OxidAV and OXavidin$_{HABA}$, compared with that of the unmodified avidin (Fig. 3*a*), indicated that combination with HABA greatly diminished the rate of tryptophan oxidation. The size exclusion chromatography analysis of avidins confirmed these results. The concentrations being equal, OxidAV, because of more extensive protein degradation, showed the shortest peak, with an absorbance 280/260 ratio of ~1.0, compared with 1.5 for OXavidin$_{HABA}$ and 1.7 for avidin. In addition, the

TABLE 2

Thermal stability comparison of avidin, OxidAV, and OXavidin$_{HABA}$ determined by circular dichroism spectroscopy before and after oxidation, with and without 4 equivalents of biotin

The *p* values are for the slope of the sigmoidal curve. NA, not applicable.

	T_m	*p*
	℃	
Avidin	79.0 ± 0.1	14.7 ± 0.3
Avidin + 4 eq biotin	>95	NA
OxidAV	74.3 ± 0.1	8.9 ± 0.1
OxidAV + 4 eq biotin	86.3 ± 0.2	20.7 ± 1.1
OXavidin$_{HABA}$	78.1 ± 0.3	11.2 ± 0.4
OXavidin$_{HABA}$ + 4 eq biotin	>95	NA

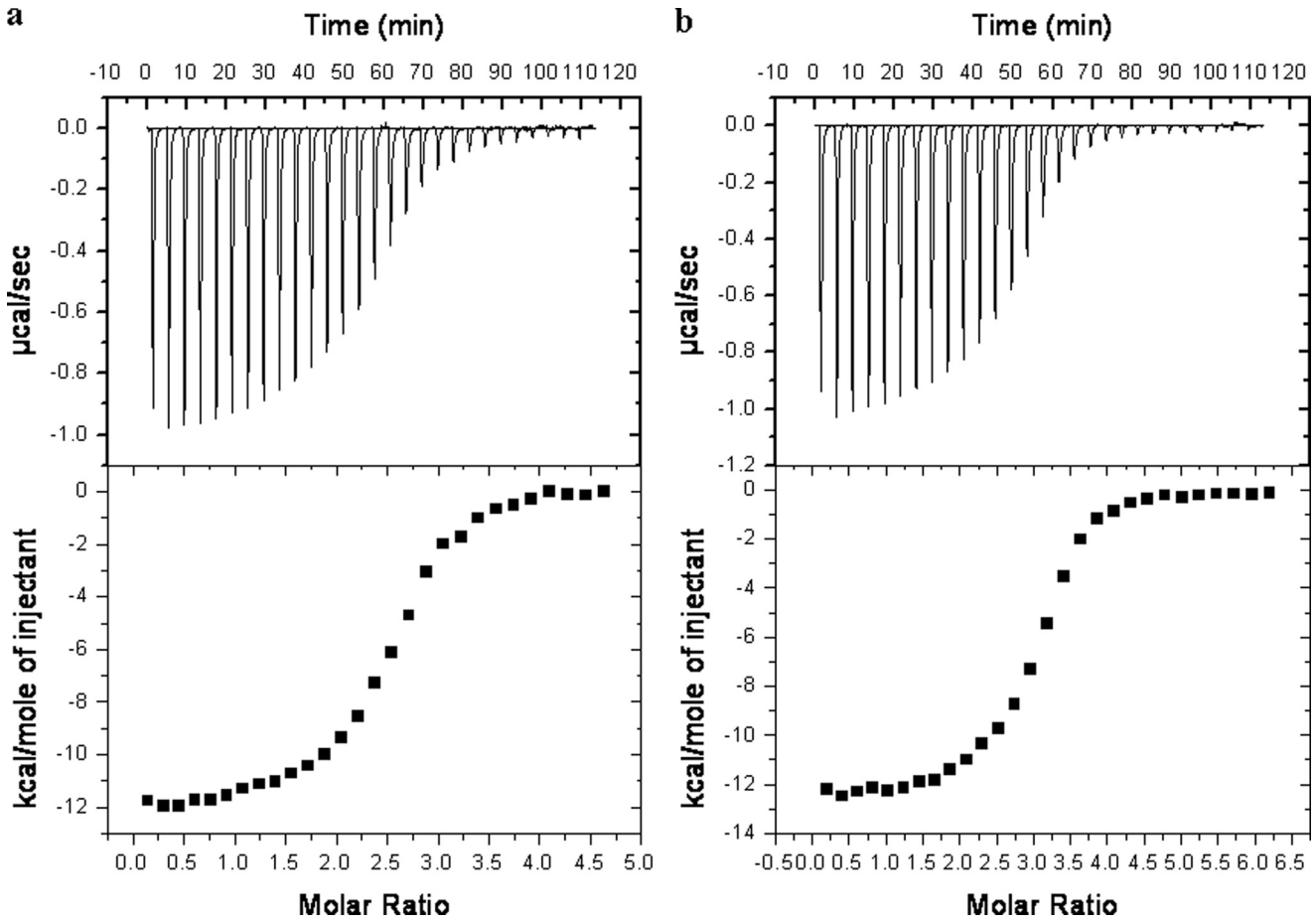

FIGURE 5. **Calorimetric titration of OXavidin$_{HABA}$ (*a*, *top panel*) and avidin (*b*, *top panel*) with ST2210 in sodium acetate 100 mM, pH 5.5.** The heat of dilution of ST2210 into buffer was subtracted. *Bottom panels*, enthalpy/mole of ST2210 injected *versus* ST2210/OXavidin$_{HABA}$ and avidin molar ratio, respectively.

elution time of oxidized avidins appeared slightly delayed compared with that of avidin, most likely because of modification of hydrodynamic behavior consequent to oligosaccharide oxidation (Fig. 3*b*).

In strict agreement with these findings, OXavidin$_{HABA}$ showed structural and thermodynamic properties very similar to avidin. Thermal stability and conformational changes were determined by circular dichroism spectroscopy before and after heating (Fig. 4, *top* and *bottom panels*, respectively), without and with 4 equivalents of biotin (Fig. 4, *panels a* and *b*, respectively). The data, collected in Table 2, indicated that oxidation decreased thermal stability, as determined by the lowering of the melting temperature (T_m) and of the slope (p) of the sigmoidal curve of OxidAV compared with that of native avidin (74.3 *versus* 79.0 and 8.9 *versus* 14.7 °C, respectively). Nevertheless, the destabilization effect of oxidation was almost totally inhibited by incubation of avidin with HABA, as confirmed by the T_m and p values of OXavidin$_{HABA}$ and avidin, corresponding to 78.1 *versus* 79.0 and 11.2 *versus* 14.7 °C, respectively. Although thermal denaturation was irreversible for both OxidAV and OXavidin$_{HABA}$ when heated without biotin, only OXavidin$_{HABA}$ retrieved its secondary structure, similarly to avidin, when heated/cooled in the presence of biotin. These findings confirm that the occupancy of biotin-binding sites by HABA preserved the conformation of avidin subjected to chemical oxidation and explain the consequently retained biotin binding capacity.

TABLE 3

Thermodynamic parameter comparison of avidin, OxidAV, and OXavidin$_{HABA}$ interaction with ST2210, determined by isothermal titration calorimetry

	N	K	Δ*H*	Δ*S*
		M^{-1}	*cal mol*$^{-1}$	*cal mol*$^{-1}$ *K*$^{-1}$
Avidin	3.0 ± 0.016	3.45E6 ± 3.07E5	−1.48E4 ± 114.0	−19.6
OxidAV	1.2 ± 0.012	6.45E5 ± 5.69E4	−0.79E4 ± 117.8	0.16
OXavidin$_{HABA}$	2.5 ± 0.015	2.69E6 ± 2.74E5	−1.163E4 ± 98.4	−9.60

Evaluation of thermodynamic parameters determined by titration of avidins with ST2210, by means of isothermal titration calorimetry (Fig. 5), underlines that ST2210 was able to bind to OXavidin$_{HABA}$ and avidin (*a* and *b*, respectively) in a comparable manner, because the association constants (K_A) and enthalpy change (Δ*H*) were of the same magnitude, whereas the ST2210/OxidAV interaction showed, as expected, lower K_A and higher Δ*H* (Table 3). According to data of ST2210 binding to oxidized avidins, within experimental error, the determined stoichiometry of interaction is 3.0, 1.2, and 2.5 molecules of ST2210/molecule of avidin, OxidAV, and OXavidin$_{HABA}$, respectively.

Residency of Oxidized Avidin in Tissue and Uptake of ^{111}In-ST2210—To evaluate the potential of oxidized avidin for therapeutic applications, the chemical hypothesis that this

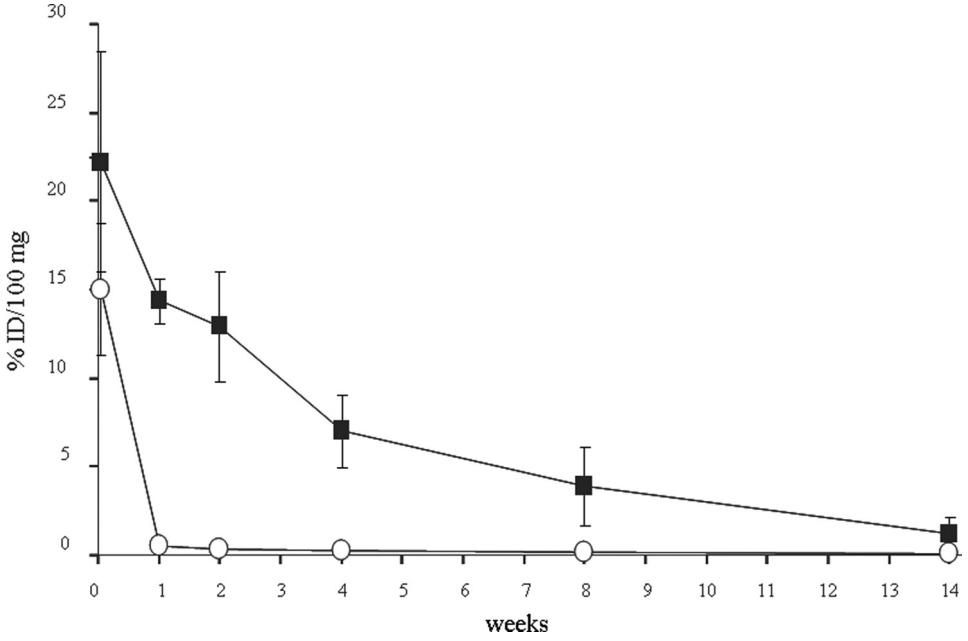

FIGURE 6. **Long term kinetics of ^{125}I-labeled avidin (○) and OXavidin$_{HABA}$ (■) after intramuscular injection in the limb of Balb/c mice.** At the indicated time points the mice were sacrificed, and samples of treated limb were weighed and counted in a γ counter. The data are expressed as the percentages of injected dose/100 mg (% ID/100 mg) of tissue. Each point corresponds to the average of five mice. The *bars* represent standard deviations.

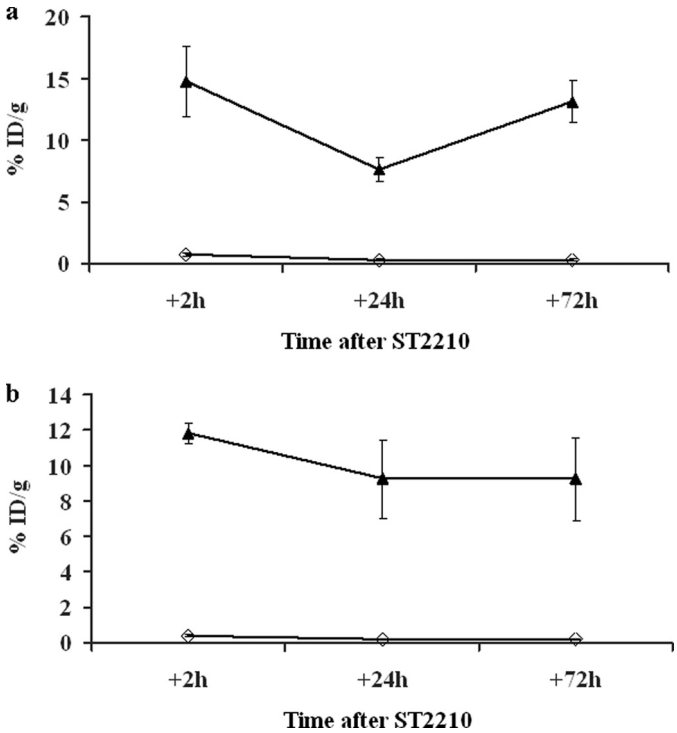

FIGURE 7. **Uptake of ^{111}In-ST2210 in the muscular limb pretreated 16 (*a*) or 48 (*b*) h earlier with avidin (◇) or OXavidin$_{HABA}$ (▲).** The mice were sacrificed 2, 24, or 72 h after intravenous injection of ^{111}In-ST2210, and samples of treated limb were weighed and counted in a γ counter. The data are expressed as the percentages of injected dose/g (% ID/g) of tissue. Each point is the average of five mice. The *bars* represent standard deviations. This result confirms OXavidin$_{HABA}$ tissue stability and shows its capacity to uptake and keep bound the radioactive biotin.

modified avidin would interact with tissue proteins and remain longer than native avidin in a treated tissue was further investigated by injecting ^{125}I-labeled avidin or OXavidin$_{HABA}$ in the muscle of one hind limb of each mouse, as described previously. At the indicated time points, the mice were sacrificed to measure the radioactivity in the treated limb as well as in other nontarget organs.

The results in Fig. 6 indicate that the half-life of OXavidin$_{HABA}$ in the treated limb is ~2 weeks as opposed to ~2 h previously reported for avidin (35). Both avidins were almost undetectable in blood, liver, and kidney 2 days after the intramuscular injection (data not shown).

The significantly higher tissue residence of OXavidin$_{HABA}$ compared with avidin in the injected limb is paralleled by a higher uptake of ^{111}In-ST2210 injected intravenously 16 or 48 h after the treatment with avidin and OXavidin$_{HABA}$. Groups of mice were sacrificed 2, 24, and 72 h after the injection of ^{111}In-ST2210, and the radioactivity in the treated limb was measured by a γ counter. The data in Fig. 7 show that OXavidin$_{HABA}$-treated limbs exhibited a highly efficient uptake of radiolabeled biotin, both when the radiolabeled biotin was injected 16 (*panel a*) or 48 (*panel b*) h after tissue avidination, and that the binding was stable. In the same conditions the uptake of ^{111}In-ST2210 by native avidin-treated limbs was almost negligible. The area under the curve values of this study, calculated taking into account the loss of energy caused by the spontaneous radioactive decay of ^{111}In, after 16 and 48 h were 19.2 *versus* 529.8 and 11.8 *versus* 498.6 for avidin and OXavidin$_{HABA}$, respectively.

Considering that polyethylene glycol (PEG) conjugation of avidin was previously attempted to improve its pharmacokinetic and biodistribution properties (27, 46) and to investigate the extraordinary tissue binding properties of oxidized avidin, ^{125}I-PEG-avidin (hydrazone) was previously produced by reacting CHO groups of ^{125}I-oxidized avidin with a molar excess of 10-kDa PEG-hydrazide. After purification by size exclusion chromatography, ^{125}I-PEG-avidin was injected in the muscle of mice as described previously, and its tissue residence was compared with the one of radiolabeled avidin and oxidized avidin. The results indicated that 24 h after injection, less than 2% ID/100 mg of PEG-avidin and avidin was present in the treated limb *versus* ~16% of oxidized avidin (35). These findings, besides ruling out the possibility of improving the tissue permanence of avidin simply by increasing its size as for intravenously injected PEG-avidin, provide further evidence of the relationship between oxidized avidin tissue permanence and aldehyde groups.

DISCUSSION

With the aim of promoting a stable binding of avidin to target tissues, we have previously investigated the feasibility of

exploiting the sugar pyranosidic rings of avidin to generate reactive groups (35). Therefore, according to the well known and specific method that allows the generation of reactive aldehydes on the carbohydrate moieties of proteins by oxidation with sodium periodate (40, 44), native avidin was chemically modified by means of HABA-assisted oxidative cleavage of oligosaccharides. The interaction of avidin with the benzoate ring of HABA is relatively weak ($K_d = 5.8 \times 10^{-6}$ M), but because it emulates the high affinity interaction of the protein with the ureido moiety of D-biotin ($K_d = 1 \times 10^{-15}$ M), the avidin-HABA complex formation preserves, from the oxidation damage, the protein structure and its biotin binding capacity. This oxidized avidin, named $OXavidin_{HABA}$, exhibits CHO groups that are substantially inert when the product is formulated at acidic pH but that react with NH_2 groups at neutral pH to form bases of Schiff. Interestingly, the formation of Schiff's bases involving oxidized avidin occurs with living cells and tissue proteins, and this interaction results in a tissue half-life of 2 weeks, compared with 2 h for native avidin. The overall biochemical profile of $OXavidin_{HABA}$ describes a product, free or complexed to biotinylated therapeutics (35), exhibiting, by Purpald's method, 8–15 active CHO groups/molecule, generated by oxidation with sodium periodate.

Regarding the biochemical characterization, $OXavidin_{HABA}$ shows spectroscopic properties similar to that of native avidin, indicating that tryptophan residues are spared from oxidation damage. In strict agreement with these results, circular dichroism and isothermal titration calorimetry analyses confirm that HABA-assisted oxidation prevents the destabilization effect because of the periodate oxidation, as demonstrated by the highly efficient binding of biotin.

A lot of effort has been recently devoted to the development of targeted delivery systems for brachytherapy (brachios, in Greek meaning short, refers to radiotherapy of tumors by contact), including biodegradable dextran or chitosan hydrogels (47, 48). The avidin property of spontaneous association to boric acid gel suspension has been exploited to promote binding of avidin to tumor cells *in vivo* (49). A fusion protein named Scavidin consisting of the macrophage scavenger receptor class A and avidin, which was shown to be binding and being internalized by tumor cells (50), an avidin/biotin liposome system for peritoneal delivery (51), and avidin bioconjugate with thermoresponsive polymer (52) were also described previously.

The use of oxidized avidin may offer a number of potential advantages also compared with current brachytherapy devices like permanent radioactive seeds (53, 54), catheters (55, 56), balloons (57, 58), or other modified avidins. For instance, the perfusion of a target tissue with $OXavidin_{HABA}$ could allow the delay by several days of the administration of biotinylated therapeutics whenever the patient conditions or the logistics might recommend it or fractionation of the therapeutic dose with no need to immobilize the treated tissue, as for example, in current seeds brachytherapy to prevent migration of the seeds. Moreover, because most of the injected $OXavidin_{HABA}$ binds and resides in the treated tissue, it will be not necessary to perform a chasing step with biotinylated albumin to block biotin uptake in nontarget organs.

It should also be taken into consideration that the formation of Schiff's bases between oxidized sugars and protein NH_2 groups is a common event *in vivo*, leading to protein glycation (59). Moreover, hundreds of oxidized proteins have been recently characterized in the plasma of animals as the common product of oxidative stress (60, 61). In addition, it is noteworthy that the use of HABA for the preparation of $OXavidin_{HABA}$ for human use is convenient because such low affinity, nontoxic ligand can be easily removed by simple dialysis or chromatography. Preclinical safety and immunogenicity studies with $OXavidin_{HABA}$ are ongoing in both rodents and nonhuman primates showing good local and systemic tolerability.[3]

Overall, we believe that $OXavidin_{HABA}$ is a promising device that, for its peculiar features, exhibits an extraordinary potential for a variety of therapeutic applications if used with different biotinylated agents like radioisotopes, chemotherapeutics, growth factors, plasmids, viral vectors, effector, or stem cells. Therefore, besides cancer, $OXavidin_{HABA}$ might be employed for directing biotinylated therapeutics to different tissues for the cure of inflammatory, autoimmune, degenerative, or genetic diseases.

Acknowledgments—We thank Prof. Giovanni Cassani and Dr. Gilles Pain for critical reading of the manuscript and suggestions.

REFERENCES

1. Green, N. M. (1990) *Methods Enzymol.* **184,** 51–67
2. Wilchek, M., and Bayer, E. A. (1990) *Methods Enzymol.* **184,** 5–13
3. Hnatowich, D. J., Virzi, F., and Rusckowski, M. (1987) *J. Nucl. Med.* **28,** 1294–1302
4. Sakahara, H., and Saga, T. (1999) *Adv. Drug Deliv. Rev.* **37,** 89–101
5. Oehr, P., Westermann, J., and Biersack, H. J. (1988) *J. Nucl. Med.* **29,** 728–729
6. Paganelli, G., Malcovati, M., and Fazio, F. (1991) *Nucl. Med. Commun.* **12,** 211–234
7. Veyrat-Follet, C., Vivier, N., Trellu, M., Dubruc, C., and Sanderink, G. J. (2009) *J. Thromb. Haemost.* **7,** 559–565
8. Green, N. M. (1975) *Adv. Protein Chem.* **29,** 85–133
9. Subramanian, N., and Adiga, P. R. (1997) *Biochem. Mol. Biol. Int.* **43,** 375–382
10. DeLange, R. J. (1970) *J. Biol. Chem.* **245,** 907–916
11. Bruch, R. C., and White, H. B., 3rd (1982) *Biochemistry* **21,** 5334–5341
12. Hiller, Y., Gershoni, J. M., Bayer, E. A., and Wilchek, M. (1987) *Biochem. J.* **248,** 167–171
13. Hubbard, A. L., Wilson, G., Ashwell, G., and Stukenbrok, H. (1979) *J. Cell Biol.* **83,** 47–64
14. Ashwell, G., and Harford, J. (1982) *Annu. Rev. Biochem.* **51,** 531–554
15. Townsend, R., and Stahl, P. (1981) *Biochem. J.* **194,** 209–214
16. Toth, C. A., Thomas, P., Broitman, S. A., and Zamcheck, N. (1982) *Biochem. J.* **204,** 377–381
17. Pimm, M. V., Fells, H. F., Perkins, A. C., and Baldwin, R. W. (1988) *Nucl. Med. Commun.* **9,** 931–941
18. Rosebrough, S. F. (1993) *Nucl. Med. Biol.* **20,** 663–668
19. Rosebrough, S. F., and Hartley, D. F. (1996) *J. Nucl. Med.* **37,** 1380–1384
20. Schechter, B., Silberman, R., Arnon, R., and Wilchek, M. (1990) *Eur. J. Biochem.* **189,** 327–331
21. Marshall, D., Pedley, R. B., Melton, R. G., Boden, J. A., Boden, R., and Begent, R. H. (1995) *Br. J. Cancer* **71,** 18–24
22. Yao, Z., Zhang, M., Sakahara, H., Nakamoto, Y., Higashi, T., Zhao, S., Sato,

[3] F. Petronzelli, A. M. Anastasi, A. Pelliccia, C. Albertoni, A. Rosi, B. Leoni, V. D'Alessio, E. Nucera, C. Chiapparino, M. L. Pacello, M. Rossi, A. Verdoliva, and R. De Santis, manuscript in preparation.

N., Arano, Y., and Konishi, J. (1999) *J. Nucl. Med.* **40,** 479–483
23. Schechter, B., Arnon, R., Colas, C., Burakova, T., and Wilchek, M. (1995) *Kidney Int.* **47,** 1327–1335
24. Knox, S. J., Goris, M. L., Tempero, M., Weiden, P. L., Gentner, L., Breitz, H., Adams, G. P., Axworthy, D., Gaffigan, S., Bryan, K., Fisher D. R., Colcher, D., Horak I. D., and Weiner L. M. (2000) *Clin. Cancer Res.* **6,** 406–414
25. Schellekens, H. (2002) *Clin. Ther.* **24,** 1720–1740
26. Weiden, P. L., and Breitz, H. B. (2001) *Crit. Rev. Oncol. Hematol.* **40,** 37–51
27. Chinol, M., Casalini, P., Maggiolo, M., Canevari, S., Omodeo, E. S., Caliceti, P., Veronese, F. M., Cremonesi, M., Chiolerio, F., Nardone, E., Siccardi, A. G., and Paganelli, G. (1998) *Br. J. Cancer* **78,** 189–197
28. Meyer, D. L., Schultz, J., Lin, Y., Henry, A., Sanderson, J., Jackson, J. M., Goshorn, S., Rees, A. R., and Graves, S. S. (2001) *Protein Sci.* **10,** 491–503
29. Nardone, E., Rosano, C., Santambrogio, P., Curnis, F., Corti, A., Magni, F., Siccardi, A. G., Paganelli, G., Losso, R., Apreda, B., Bolognesi, M., Sidoli, A., and Arosio, P. (1998) *Eur. J. Biochem.* **256,** 453–460
30. Marttila, A. T., Airenne, K. J., Laitinen, O. H., Kulik, T., Bayer, E. A., Wilchek, M., and Kulomaa, M. S. (1998) *FEBS Lett.* **441,** 313–317
31. Marttila, A. T., Laitinen, O. H., Airenne, K. J., Kulik, T., Bayer, E. A., Wilchek, M., and Kulomaa, M. S. (2000) *FEBS Lett.* **467,** 31–36
32. Murray, S., Maraveyas, A., Dougan, T., and Chu, A. C. (2002) *Biochim. Biophys. Acta* **1570,** 81–88
33. Nordlund, H. R., Laitinen, O. H., Uotila, S. T., Nyholm, T., Hytönen, V. P., Slotte, J. P., and Kulomaa, M. S. (2003) *J. Biol. Chem.* **278,** 2479–2483
34. Laitinen, O. H., Nordlund, H. R., Hytönen, V. P., Uotila, S. T., Marttila, A. T., Savolainen, J., Airenne, K. J., Livnah, O., Bayer, E. A., Wilchek, M., and Kulomaa, M. S. (2003) *J. Biol. Chem.* **278,** 4010–4014
35. De Santis, R., Albertoni, C., Rosi, A., Leoni, B., Petronzelli, F., D'Alessio, V., Nucera, E., Salvatori, G., Paganelli, G., Verdoliva, A., Carminati, P., and Nuzzolo, C. A. (2010) *J. Biomed. Biotechnol.* doi:10.1155/2009/921434
36. Green, N. M. (1965) *Biochem. J.* **94,** 23C–24C
37. Paganelli, G., Ferrari, M., Cremonesi, M., De Cicco, C., Galimberti, V., Luini, A., Veronesi, P., Fiorenza, M., Carminati, P., Zanna, C., Orecchia, R., and Veronesi, U. (2007) *Breast* **16,** 17–26
38. Paganelli, G., Ferrari, M., Ravasi, L., Cremonesi, M., De Cicco, C., Galimberti, V., Sivolapenko, G., Luini, A., De Santis, R., Travaini, L. L., Fiorenza, M., Chinol, M., Papi, S., Zanna, C., Carminati, P., and Veronesi, U. (2007) *Clin Cancer Res.* **13,** 5646s–5651s
39. Paganelli, G., De Cicco, C., Ferrari, M. E., Carbone, G., Pagani, G., Leonardi, M. C., Cremonesi, M., Ferrari, A., Pacifici, M., Di Dia, A., De Santis, R., Galimberti, V., Luini, A., Orecchia, R., Zurrida, S., and Veronesi, U. (2010) *Eur. J. Nucl. Med. Mol. Imaging* **37,** 203–211
40. Zaborsky, O. R., and Ogletree, J. (1974) *Biochem. Biophys. Res. Commun.* **61,** 210–216
41. Quesenberry, M. S., and Lee, Y. C. (1996) *Anal. Biochem.* **234,** 50–55
42. Urbano, N., Papi, S., Ginanneschi, M., De Santis, R., Pace, S., Lindstedt, R., Ferrari, L., Choi, S., Paganelli, G., and Chinol, M. (2007) *Eur. J. Nucl. Med. Mol. Imaging* **34,** 68–77
43. Yao, Z., Zhang, M., Sakahara, H., Saga, T., Arano, Y., and Konishi, J. (1998) *J. Natl. Cancer Inst.* **90,** 25–29
44. O'Shannessy, D. J., and Quarles, R. H. (1987) *J. Immunol. Methods* **99,** 153–161
45. Green, N. M. (1963) *Biochem. J.* **89,** 599–609
46. Caliceti, P., Chinol, M., Roldo, M., Veronese, F. M., Semenzato, A., Salmaso, S., and Paganelli, G. (2002) *J. Control Release* **83,** 97–108
47. Van Tomme, S. R., and Hennink, W. E. (2007) *Expert Rev. Med. Devices* **4,** 147–164
48. Azab, A. K., Doviner, V., Orkin, B., Kleinstern, J., Srebnik, M., Nissan, A., and Rubinstein, A. (2007) *J. Biomed. Mater. Res. A* **83,** 414–422
49. Bench, B. J., Johnson, R., Hamilton, C., Gooch, J., and Wright, J. R. (2004) *J. Colloid Interface Sci.* **270,** 315–320
50. Lehtolainen, P., Taskinen, A., Laukkanen, J., Airenne, K. J., Heino, S., Lappalainen, M., Ojala, K., Marjomäki, V., Martin, J. F., Kulomaa, M. S., and Ylä-Herttuala, S. (2002) *J. Biol. Chem.* **277,** 8545–8550
51. Zavaleta, C. L., Phillips, W. T., Soundararajan, A., and Goins, B. A. (2007) *Int. J. Pharm.* **337,** 316–328
52. Salmaso, S., Bersani, S., Pennadam, S. S., Alexander, C., and Caliceti, P. (2007) *Int. J. Pharm.* **340,** 20–28
53. Jansen, N., Deneufbourg, J. M., and Nickers, P. (2007) *Int. J. Radiat. Oncol. Biol. Phys.* **67,** 1052–1058
54. Saito, S., Nagata, H., Kosugi, M., Toya, K., and Yorozu, A. (2007) *Int. J. Clin. Oncol.* **12,** 395–407
55. Kaufman, S. A., DiPetrillo, T. A., Price, L. L., Midle, J. B., and Wazer, D. E. (2007) *Brachytherapy* **6,** 286–292
56. Denecke, T., and Lopez Hänninen, E. (2008) *Recent Results Cancer Res.* **177,** 95–104
57. Kim, Y., Johnson, M., Trombetta, M. G., Parda, D. S., and Miften, M. (2008) *Int. J. Radiat. Oncol. Biol. Phys.* **71,** 305–313
58. Adkison, J. B., Thomadsen, B., and Howard, S. P. (2008) *Brachytherapy* **7,** 43–46
59. Thornalley, P. J., Langborg, A., and Minhas, H. S. (1999) *Biochem. J.* **344,** 109–116
60. Mirzaei, H., Baena, B., Barbas, C., and Regnier, F. (2008) *Proteomics* **8,** 1516–1527; Correction (2008) *Proteomics* **8,** 2764–2771
61. Chung, W. G., Miranda, C. L., and Maier, C. S. (2008) *Electrophoresis* **29,** 1317–1324